



Conference of Scientific Students' Associations



Computational Fluid Dynamic analysis on the thermal hydraulics of a fuel assembly of the thorium-uranium fuelled SCWR

Author: **Béla Hegyesi**

BSc Energy Engineering Student, Nuclear Energy specialization

Supervisor: **Attila Kiss**

Research assistant at BME Institute of Nuclear Techniques

2016.



Table of contents

1. Introduction	3
1.1. The thermal hydraulics of supercritical water (SCW)	3
1.2. The Supercritical-Water-Cooled Reactor (SCWR)	4
2. The task	6
3. Conception and construction	7
3.1. The thorium, as fuel	7
3.2. The cladding material	8
3.3. The thermophysical properties of supercritical water	9
4. The geometry of fuel assembly and its modelling	10
4.1. The CFX model with whole circumference	10
4.2. The CFX model with one-twelfth circumference	11
5. The generation of numerical mesh (Meshing)	13
5.1. The meshing of the solid domains	13
5.2. The meshing of the fluid domains	13
5.2.1. The dimensionless wall distance (y^+)	14
6. Boundary conditions	16
6.1. CFD model with whole circumference	16
6.2. CFD model with one-twelfth circumference	17
7. Calculations	20
8. Results of the model with whole circumference	21
9. Results of the model with one-twelfth circumference	24
10. Summary	27
Bibliography	28



1. Introduction

Today’s energy industry faces new challenges in a continuously changing market environment. Energy industry should deliver more energy than ever with even more environmental restrictions. The net efficiency of power plants became highly important in the last decades. Efficiency is determined by different factors, but the efficiency of the thermodynamic cycle is determined by the temperature of which the heat enters the engine and the temperature of the environment into which the engine exhausts its waste heat. One method to increase the efficiency of a power plant is to increase the inlet temperature of the turbine, which converts the heat energy into mechanical work. Use of supercritical Rankine-cycle with higher temperatures promises a better efficiency (~44%) [1].

In my ongoing research, I deal with numerical calculations in order to investigate the thermal hydraulics of supercritical water in a new, thorium fuelled reactor concept proposed by Professor Csom. In the rest of this chapter, I shortly introduce the investigated coolant, its special features and the Supercritical-Water-Cooled Reactor (SCWR).

1.1. The thermal hydraulics of supercritical water (SCW)

Supercritical water is widely used in the technical life. Because of the advantageous thermal features of this fluid, it is a possible coolant for advanced nuclear reactors. Around the critical and pseudocritical temperatures, the thermophysical properties of supercritical water become strongly non-linear. In the pseudo-critical transition of the SCW its properties change from a liquid-like state to a vapour-like state (Figure 1). In this region, the properties of the fluid change rapidly (Figure 2).

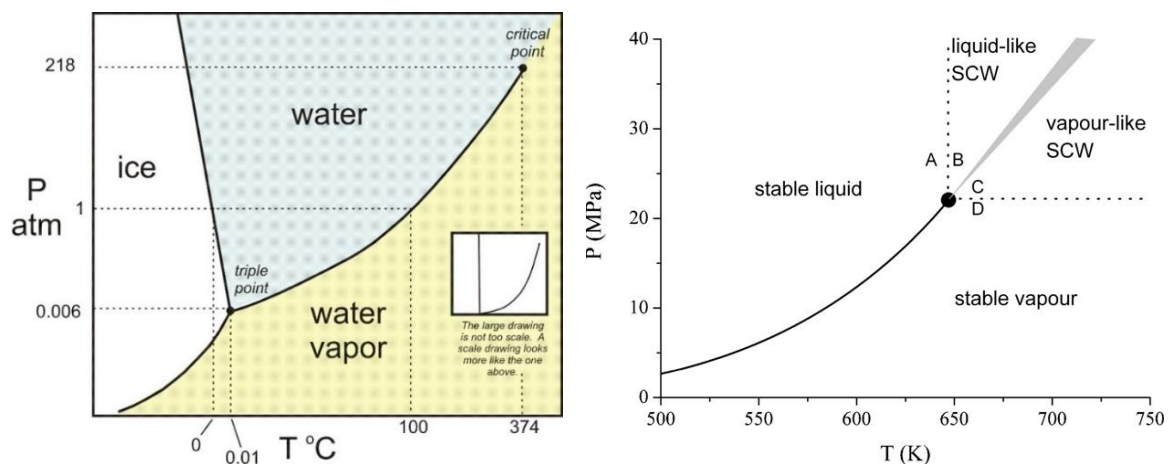


Figure 1: Phase diagram of water and the illustration of the liquid like and vapour-like SCW [2][3]



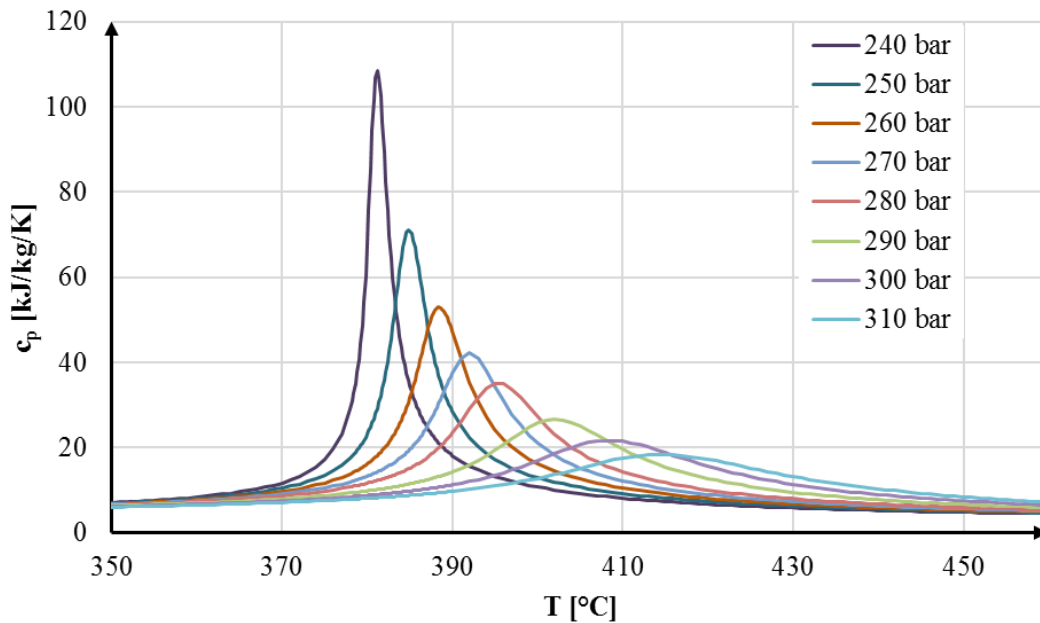


Figure 2: Isobar specific heat capacity of supercritical water at different pressures (based on the IAPWS-IF97 properties of water and steam)

In subcritical fluids at saturation temperature a first order phase change happens, while in supercritical fluids a second order phase change occurs. Second order phase transitions are also called continuous phase transitions. As its name implies, it is a continuous way instead of the fast changes of first order phase change [4] [5].

Deterioration of heat transfer (DHT) can happen under certain circumstances. It is a dangerous phenomenon (but less dangerous than the departure from nucleate boiling (DNB)) which occurs at high heat fluxes to mass flux ratios. It can lead to locally high wall temperature, and decreased (deteriorated) heat transfer [6].

1.2. The Supercritical-Water-Cooled Reactor (SCWR)

The Supercritical-Water-Cooled Reactor (SCWR) is one of the six main research directions considered in the Generation IV International Forum (GIF) [1]. This type of nuclear reactor operates above the critical pressure of water. Its coolant and moderator are also light-water and the neutron spectrum can be fast or thermal spectrum, depending on the core design [1]. The water becomes supercritical fluid in the reactor core when it reaches the pseudocritical temperature. SCWRs can reach 45% thermal efficiency, which is high in comparison with today's LWRs (~33%) [1]. As shown in Figure 3, the concept of SCWR is quite simpler compared to current PWR or BWR designs. The SCWR has simpler steam cycle



without steam generators, steam separators and with smaller primary coolant pumps. With simpler design and higher efficiency, the advantages of SCWRs are evident [1].

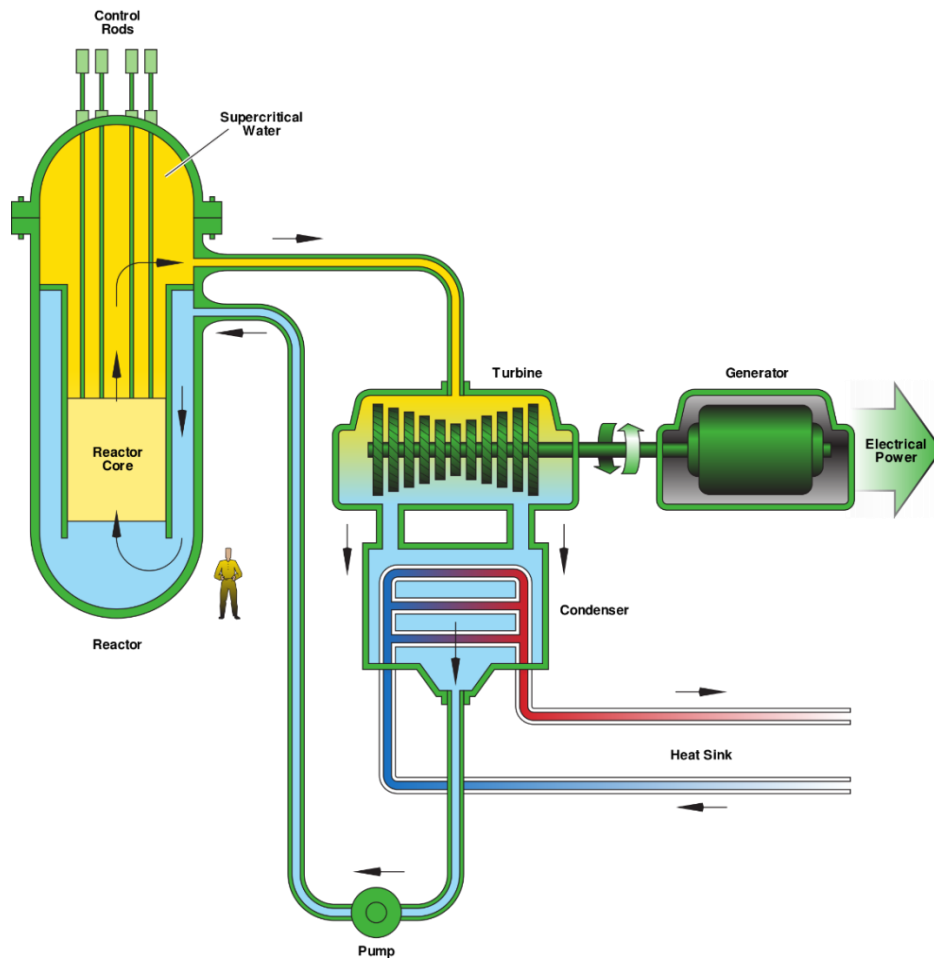


Figure 3: The concept of the SCWR [1]

Now, supercritical fossil fuel plants are in operation, and there are also supercritical and ultra-supercritical steam turbines. These turbines can handle steam up to 285 bar and 620°C [7].



2. The task

The task was to analyze an SCWR concept from a thermal hydraulics point of view. This idea was proposed by Professor Gyula Csom, examined and optimized from the reactor physics side by Dr. Tibor Reiss. He carried out a coupled neutronics – very simple (one dimensional) thermal hydraulic analysis in his Ph.D. thesis [8]. Here, the thermal hydraulic side was very simple and thus far from reality which strongly limited the applicability of the reached results of the coupled calculations. The next logical step to investigate the existing parts of this reactor concept (mainly the reactor core) is to perform more sophisticated coupled neutronics - three dimensional, thermal hydraulic, computational fluid dynamic (CFD) analysis to prove or disprove the feasibility of this concept. Dr. Tibor Reiss optimized the conception from a neutronics and burnup point of view, and proved, that a high burnup is achievable with thorium, as fuel without refuelling.

The main aim of this study was to discover the thermal hydraulics in the thorium SCWR concept by CFD calculations, specify the maximum fuel temperature and investigate the feasibility of this concept from a thermal hydraulic point of view. Another goal was to collaborate with a physicist student (who did the neutronic calculations) and work with him on this specific problem, which requires a multi-perspective approach. We had to cooperate to get the best results with the connection of MCNP (Monte-Carlo N-Particle code) and the ANSYS CFX CFD code. Initially, we worked separately on our models and methods. After we became familiar with our software we started to connect the two sides simply to share our results and use each other's results as initial and boundary conditions.

First, I created a whole fuel assembly model with a height of 210 mm in order to learn the way how complex CFD models can be built in the ANSYS CFX program and to investigate the cross-flows between the sub-channels and the possible asymmetries of the flow pattern. After the evaluation of the results of this model, I found that there are no significant asymmetries (even if in that region which was investigated with my first model), so a one-twelfth model can be used to investigate the coolant flow along the whole heated length of the fuel assembly.



3. Conception and construction

Professor Csom came to the conclusion that the $(\text{Th}^{233}\text{U})\text{O}_2$ is the natural fuel of the SCWRs, which main proof is that there is no need for extra moderator in the two-pass fuel assembly configuration [8].

Parameters of the first model and the whole reactor concept can be seen in Table 1. These values were calculated by Tibor Reiss [8].

Parameter	Value	Unit
Inlet temperature	300	[°C]
Outlet temperature	500	[°C]
Feedwater mass flow rate	1619.23	[kg/s]
Total thermal power	2971.48	[MW]
Number of assemblies	397	[-]
Coolant flow rate per fuel assembly	4.078	[kg/s]
Average heat flux at the outer surface of the cladding in the inner region	523.9	[kW/m ²]
Average heat flux at the outer surface of the cladding in the outer region	264.8	[kW/m ²]

Table 1: The parameters of the first model [8]

3.1. The thorium, as fuel

As mentioned above, thorium can be the natural fuel of SCWRs. It has several advantages but some challenges, too. It can produce less nuclear waste than today's uranium-fuelled PWRs and reach the same or higher burnup. One of the biggest advantage of the analysed construction is its simplicity, but the feasibility of this simpler concept is not confirmed for example from thermal hydraulic point of view. It is a two-pass core, where the coolant flows upwards in the inner region of the fuel assembly, and downstream in the outer region, shown in Figure 4.

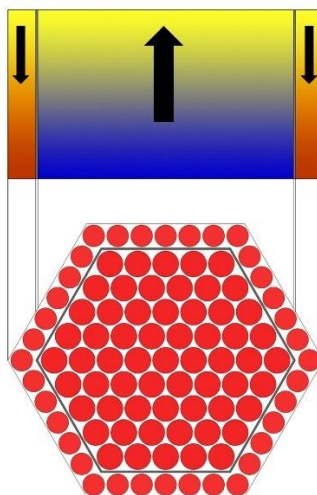


Figure 4: The flow path within the fuel assembly [8]

It is known that ^{232}Th is a better fertile isotope than plutonium. Fertile isotope is an isotope, which is not fissionable by thermal neutrons but can be converted into a fissile material by neutron absorption and subsequent nuclei conversions. It can absorb a neutron and produce ^{233}U . The exact composition of the fuel is shown in Table 2.

O_2	^{233}Th	^{235}U
0.6666	0.3666	0.02667

Table 2: The core densities of the MOX fuel

Thorium-dioxide has a higher melting point (3200-3300°C) and thermal conductivity than uranium-dioxide, but it is also decreasing as a function of temperature (Figure 5). Specific heat capacity also shown on this figure [9][10][11].

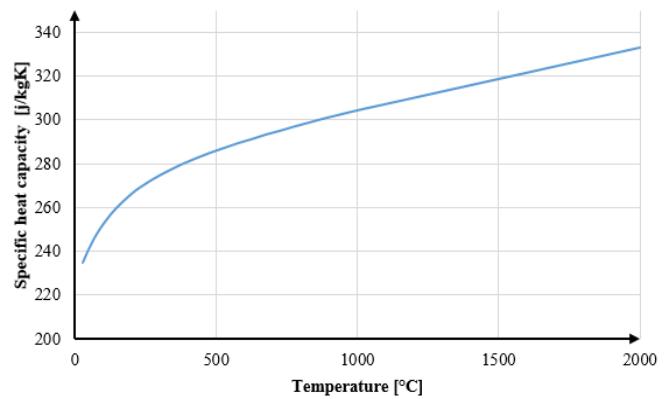
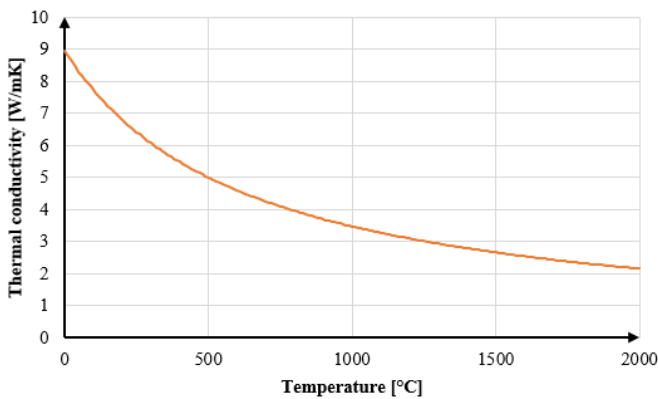
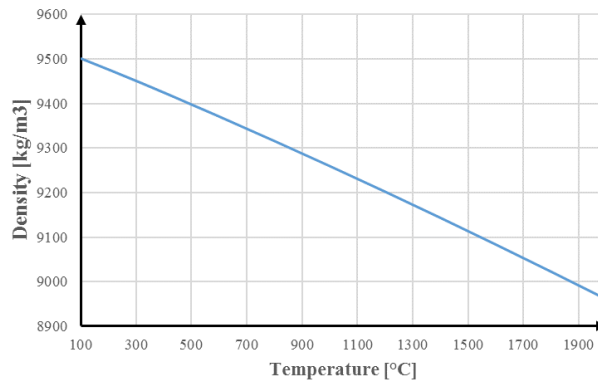


Figure 5: The density, thermal conductivity and isobar specific heat of thorium-dioxide [9]

3.2. The cladding material

SS316L stainless steel was selected for clad material. It is the low-carbon version of 316 stainless steel, and it has some advantageous property, such as corrosion resistance. The exact composition is shown in Table 3. The most important thermophysical properties of SS316L stainless steel are shown in Figure 6.



Material	Type 316L [%]
Carbon	0.03 max.
Manganese	2.00 max.
Phosphorus	0.045 max.
Sulphur	0.03 max.
Silicon	0.75 max.
Chromium	16.00-18.00
Nickel	10.00-14.00
Molybdenum	2.00-3.00
Nitrogen	0.10 max.
Iron	Balance

Table 3: The composition of SS316L stainless steel [12]

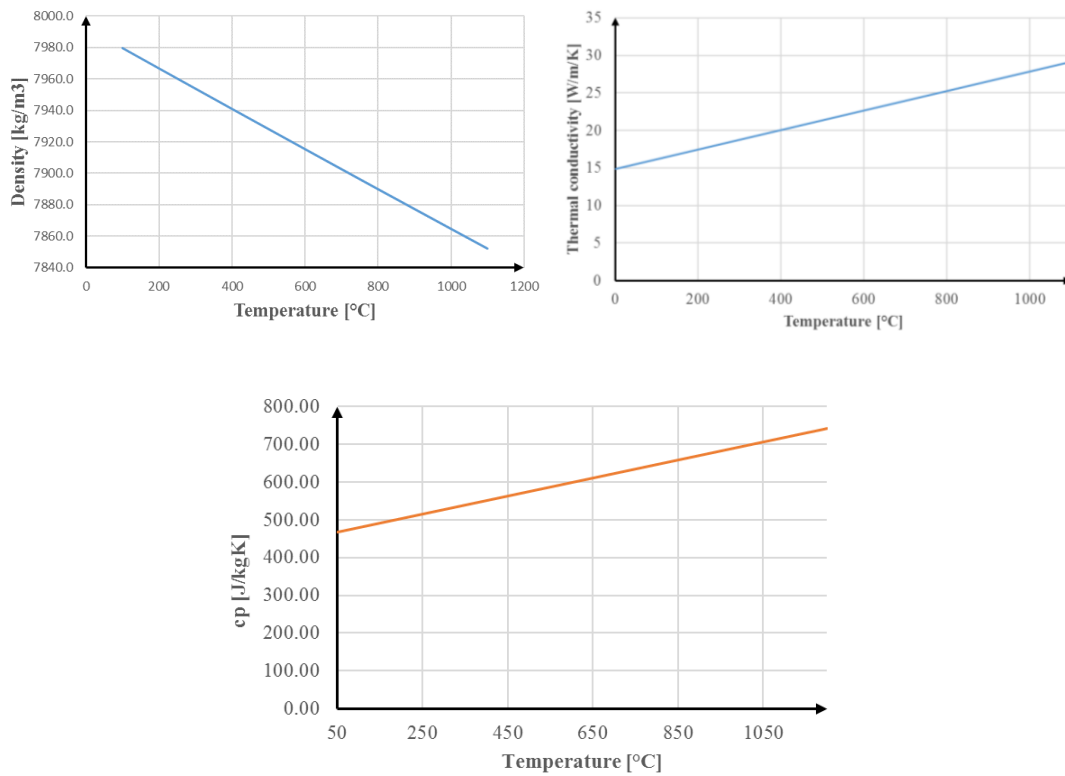


Figure 6: The density, thermal conductivity and isobar specific heat capacity of SS316L [12]

3.3. The thermophysical properties of supercritical water

I defined the supercritical water as user fluid in the ANSYS CFX Pre 17 using the IAPWS-IF97 built in material database [13] [14] [15].



4. The geometry of fuel assembly and its modelling

I used the geometrical data from Tibor Reiss's dissertation [8] to build a model of the fuel assembly. There was enough information to build a geometry without mixing chambers and spacers. I made a simple 2D drawing (Figure 7). Diameter of fuel pins are 13 mm in the inner region and 10.7 mm in the outer region. I draw the whole geometry in ANSYS ICEM. This is not the best or more comfortable 3D modelling software but its models are fully compatible with ANSYS CFX and it is a very powerful meshing software as well.

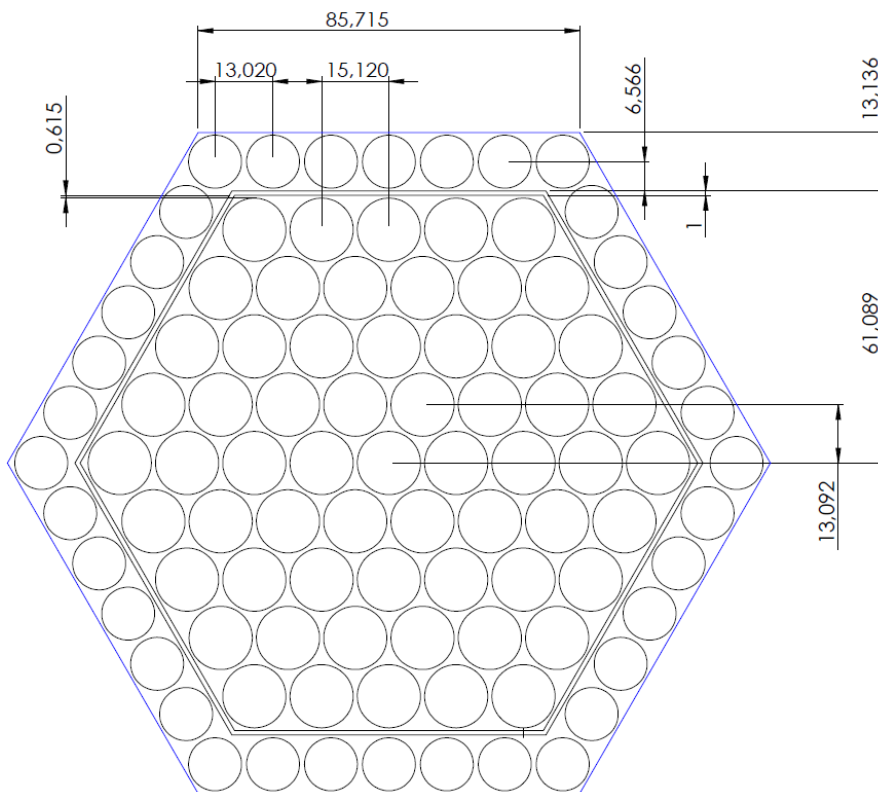


Figure 7: The cross section of the fuel assembly with its dimensions

4.1. The CFX model with whole circumference

Due to limited calculation resources, we had to choose some simplification. The first idea was to modelling a 210 mm long section of the fuel assembly, one section at the bottom, one at the top and one at the hottest region. After building this model we find out that the other team who works on the neutronics of the concept needs the distribution of the water densities along the heated length (4.2 m) to calculate the exact power densities in the fuel and other parts. That is the reason why we built a second model with one-twelfth in circumferential but with the whole heated length modelled. The so-called whole perimeter



model was useful to see the symmetry of the flow field and the low values of inter-channel cross-flows.

The whole perimeter model contained the inner and outer fluid domains, the fuel, the cladding and a wall solid domain which separated the inner and outer fluid regions. The thickness of this wall was 1 mm. Gas gap of the fuel pins, filled with helium was neglected.

Figure 8 shows the numbering of the rods in the whole perimeter model in both the inner and outer fluid domains.

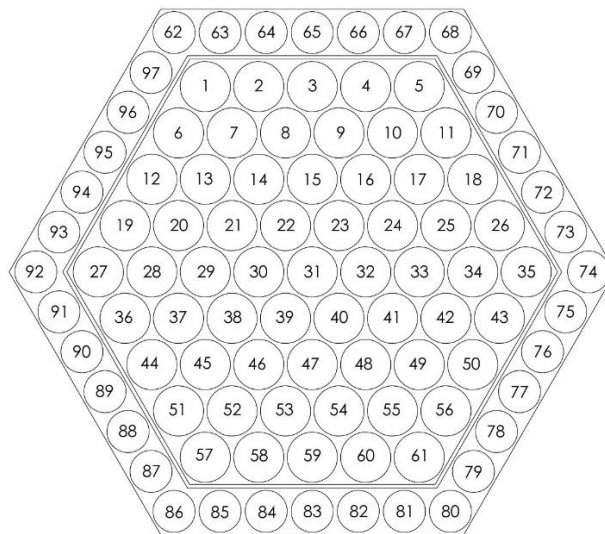


Figure 8: The numbering of the fuel rods in the first model with whole circumference

4.2. The CFX model with one-twelfth circumference

After evaluation of the first model and understanding the exact needs of physicists, building of a one-twelfth fuel assembly model for the whole length (4.2 m) was chosen. The model is shown in Figure 9. Since the whole circumference model and fortunately the flow field in it are symmetric, we can cut it into parts and modelling just the one-twelfth of its circumference (see Figure 9).



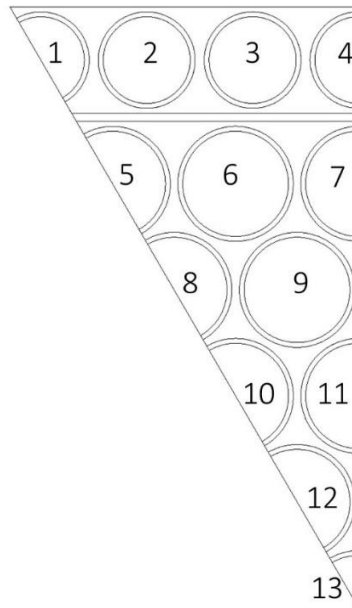


Figure 9.: The numbering of the fuel rods in the one-twelfth model

5. The generation of numerical mesh (Meshing)

I used ANSYS ICEM for meshing. After building geometry in it, it was the easiest way to create the numerical grids or meshes.

5.1. The meshing of the solid domains

I used 3D block structured hexahedral mesh in the solid domains. First, I removed every unnecessary item from the geometry and created 3D blocks around the necessary parts. After that, I used O-grids to refine the mesh and define the exact node numbers. In the whole circumference model, I used 42 axial layers (5 mm layer height). In the one-twelfth model, I used 1000 layers (4.2 mm layer height).

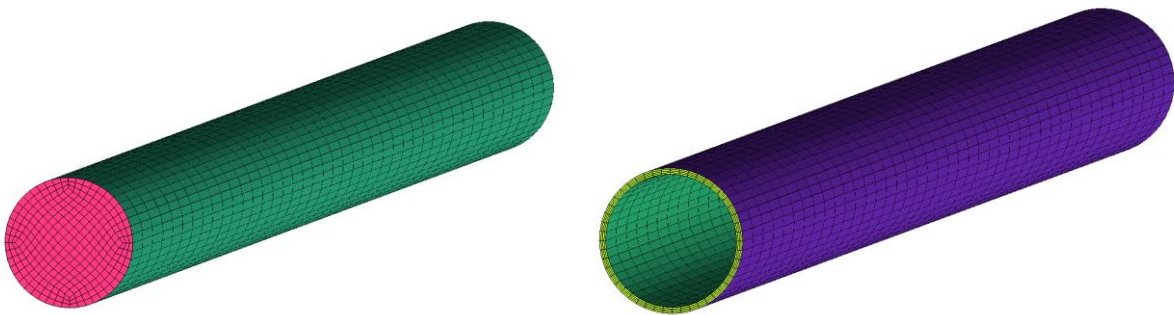


Figure 10: The numerical meshes of a fuel and a cladding of the inner region

5.2. The meshing of the fluid domains

I generated extruded meshes for the two fluid domains by the following method. I scaled down the geometry (typically to 1/20 – 1/1000 of the original size in Z-axis direction) then meshed with the ICEM and deleted every mesh except the surface mesh on outlet or inlet (see Figure 11) – depended on their mesh quality. I used densities to refine the mesh in the critical regions, mainly in gaps. Then I simply extruded the inlet or outlet surface mesh in Z-axis direction using appropriate number of layers.



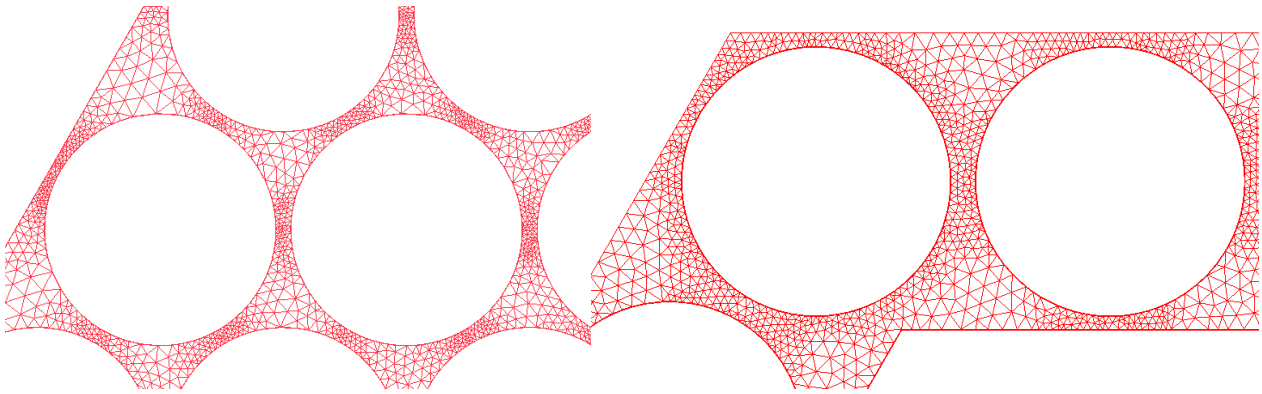


Figure 11: Mesh of the fluids in the inner (on the left) and outer (on the right) region in the whole circumference model

5.2.1. The dimensionless wall distance (y^+)

One of the most important dimensionless numbers in numerical simulation is the dimensionless wall distance between the wall and the first node nearest to the wall (called as “ y_1^+ ” or “y plus” in ANSYS terminology [15]).

The dimensionless wall distance is used more generally in fluid dynamics and CFD: y^+ is commonly used in boundary layer theory (for e.g. in defining the law of the wall) [16]. The non-dimensional wall distance for a wall-bounded flow can be defined in the following way:

$$y^+ = \frac{u_\tau \Delta y}{\nu}$$

u_τ : friction velocity at the nearest wall [m/s],

Δy : the distance to the nearest wall [m],

ν : local kinematic viscosity of the fluid [m²/s].

$$u_\tau = \sqrt{\frac{\tau_w}{\rho}}$$

τ_w : wall shear stress [Pa]

ρ : density of the fluid [kg/m³]

I created a first mesh, to analyse the value of y plus (see Figure 12). As Figure 12 shows, the expansion factor between the last layer of the near wall prism mesh and the bulk tetra mesh seems to be too large. I tried to optimize this transition between the two parts of the mesh, but I did not succeed due to computer hardware limitations (the model has run out of



available RAM memory). In the future, I plan to optimize the numerical mesh to solve this problem.

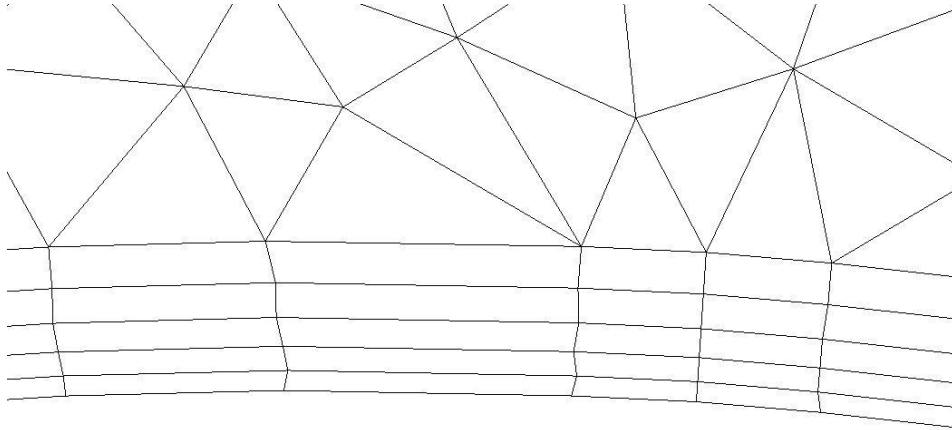


Figure 12: Illustration of prism layers next to the surface of a cladding

After the first test calculation, the value of y plus in the inner region was 23.2, and in the outer was 65. These are high values, so I decreased the height of the first prism layer to achieve the desired y plus value (around or less than 1). The achieved y plus values are shown in Table 4.

Parameter	Inner fluid	Outer fluid
height of first layer [mm]	0.001	0.0004
number of layers [-]	7	12
height ratio [-]	1.3	1.3
y_1^+ [-] (average)	0.86	0.86

Table 4: The near wall mesh parameters of the prism layers in the model with whole circumference

In the one-twelfth model for the whole length y plus values are higher, but they are still in an acceptable range. They are shown in Table 5.

Parameter	Inner fluid	Outer fluid
height of first layer [mm]	0.0008	0.0004
number of layers [-]	6	8
height ratio [-]	1.3	1.3
y_1^+ [-] (average)	1.4-1.6	1

Table 5: The near wall mesh parameters of the prism layers in the one-twelfth model



6. Boundary conditions

In this chapter I describe the details of applied boundary conditions for both CFD models.

6.1. CFD model with whole circumference

In the first analysis, turbulence model in fluids was SST (Shear Stress Transport), which is the best two equation model. The most important boundary details are shown in Table 6 and 7. The used meshes of inlet and outlet regions are shown in Fig. 9 and 10. These meshes was extruded (50 layers, 4.2 mm axial height).

Property	Unit	Inner fluid	Outer fluid
Material	-	SCW	SCW
Inlet temp.	[°C]	300	496.25
Reference pressure	[bar]	250	250
Inlet abs. pressure (calculated)	[bar]	250.034	250.117
Outlet absolute pressure	[bar]	250	250
Pressure profile blend (outlet)	[-]	0.05	0.05
Heat transfer	-	Total energy	Total energy
Mass flow rate	[kg/s]	4.078	4.078
Turbulence model	-	SST	SST
Turbulence	-	Medium (Intensity=5%)	Medium (Intensity=5%)
Wall function	-	automatic	automatic
Energy source	[W/m ³]	4,775,195.45	706,195.825

Table 6: The details of the boundary conditions in case of the model with whole circumference (one exception: the inlet absolute pressure – it is here for comparison purpose only)

I am aware that the outlet absolute pressure of the inner SCW domain should be higher than the inlet absolute pressure of the outer SCW domain (see Table 6 and Table 8). At the current stage of my research, I had to use an outlet for the inner SCW domain and an inlet for the outer SCW domain to make more robust my CFD model. In the next step of this research, I will modify the model to make more realistic the CFD model. I will change these above-mentioned boundary conditions. I will connect the outlet boundary surface of inner SCW domain to the inlet boundary surface of the outer SCW domain with a general connection type fluid-fluid interface. That is how I will ensure that the absolute pressure distribution will be strictly monotonically decreasing from the inlet of inner SCW domain to the outlet of the outer SCW domain.

The six side surfaces of the model have been defined as symmetry surfaces due to the concept has an open fuel assembly design at the current state.

Property	Unit	Inner fuel	Outer fuel	Inner clad	Outer clad
Energy source	[W/m ³]	158,770,664.4	144,589,384.9	6,013,223.0	5,031,069.6

Table 7: The specified heat sources of the solid domains



6.2. CFD model with one-twelfth circumference

In the first analysis, turbulence model was k-epsilon which was served a good set of initial condition for the second and the later models, which used SST (Shear Stress Transport) turbulence model.

In the next analysis, turbulence model was SST too. Initial results of the first analysis was used. Energy sources of this model were defined by user functions (independent variable was the Z coordinate (from 0 to 4.2 m), while the dependent variable was the volumetric heat source); they were received from reactor physics calculation from András Ványi [17].

The boundary conditions of this model can be seen in Table 8.

Property	Unit	Inner fluid	Outer fluid
Material	-	SCW	SCW
Inlet temp.	[°C]	300	450
Reference pressure	[bar]	250	250
Inlet abs. pressure (calculated)	[bar]	251.08	251.687
Outlet absolute pressure	[bar]	250	250
Pressure profile blend (outlet)	[-]	0.05	0.05
Heat transfer	-	Total energy	Total energy
Mass flow rate	[kg/s]	0.33983	0.33983
Turbulence model	-	SST	SST
Turbulence	-	Medium (Intensity=5%)	Medium (Intensity=5%)
Wall function	-	automatic	automatic
Energy source	[W/m ³]	Defined by user function	Defined by user function

Table 8: The details of the boundary conditions in case of the one-twelfth model (one exception again: the inlet absolute pressure – it is here for comparison purpose only as well)

Figure 13 shows the distribution of power density (or volumetric heat source) for four different cases in the outer region, while Figure 14 shows it in the inner region.

The used power densities are shown on Figure 13 and Figure 14 [17]. The first (“Inner/Outer fuel heat source 1”) was calculated with a constant water density (for inner region: 700 kg/m³, outer region: 100 kg/m³) [17]. The second (“Inner/Outer fuel heat source 2”) was calculated after the first results of CFX calculations. Densities are shown on Figure 15. András Ványi developed a coupled one-dimensional thermal hydraulics program which calculates the average density of water in 40 axial layers and he used these densities to get better results for power densities [17]. After some iterations, his program system get the results, also shown on Figure 13 and Figure 14. “Inner/Outer fuel heat source steady state” curve shows the original results and after that I used these power density values as boundary conditions to my CFX model to calculate a more realistic CFD result. The calculated densities



of the SCW are also shown on Figure 15 as “Inner/Outer region steady state”. Using these new density distributions of SCW, András Ványi recalculated the power densities and these are the last results which can be seen in Figure 13 and Figure 14 as “Inner/Outer fuel heat source steady state 2”. This document contains the results reached up to this point of the iteration between me and András Ványi’s works.

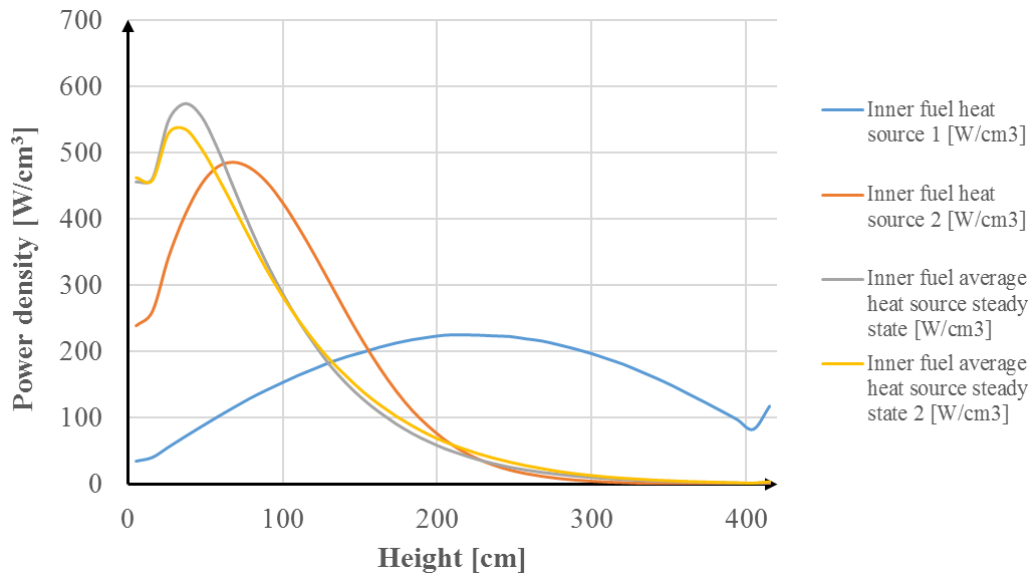


Figure 13: The distribution of the power densities in the inner region [17]

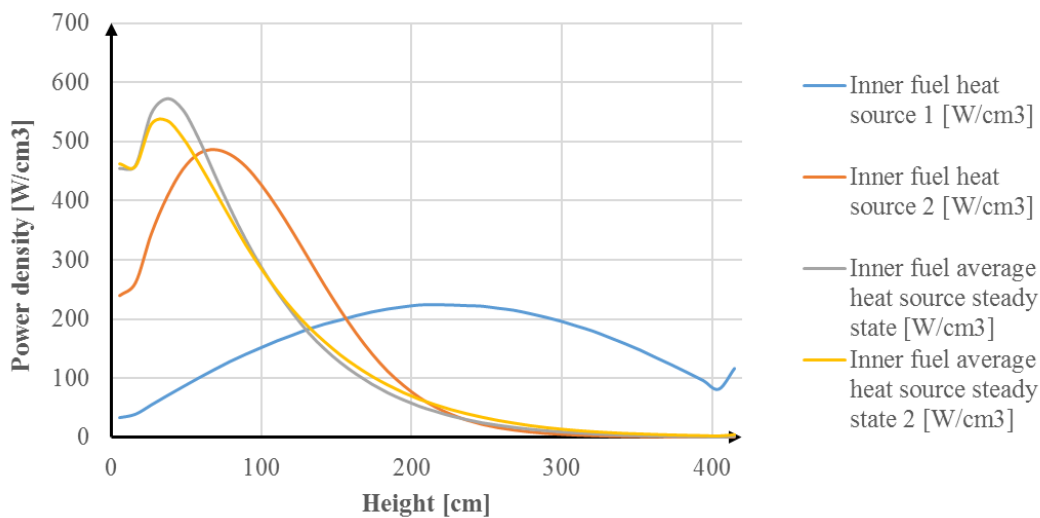


Figure 14: The distribution of the power densities in the outer region [17]



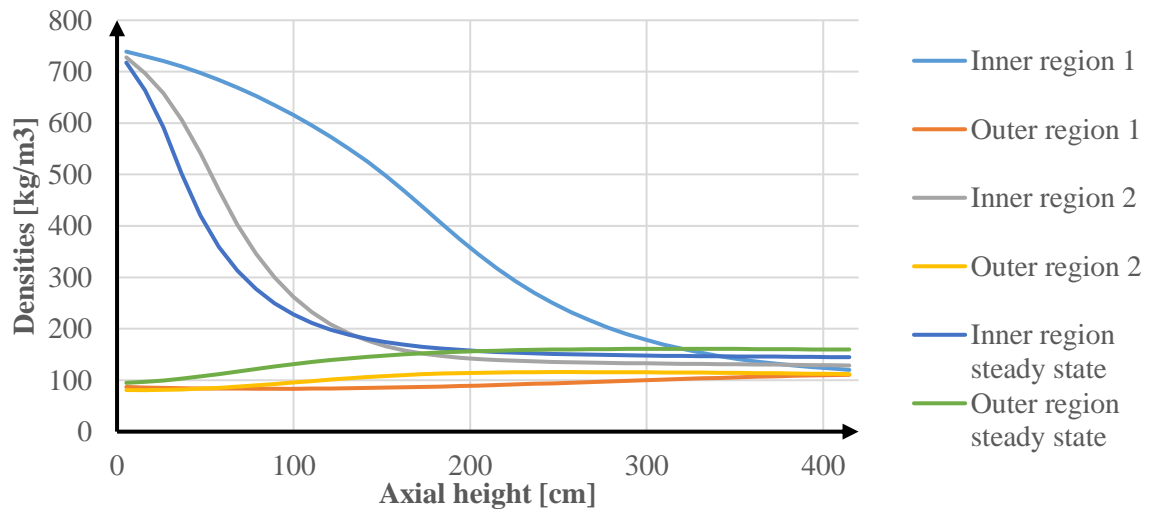


Figure 15: The axial distribution of the average density of water in the different cases and regions

7. Calculations

Calculations were carried out on PCs and on the Alfonz High-Performance Cluster at the Institute of Nuclear Techniques. ANSYS CFX-Solver Manager 17.0 was used to run the simulations and ANSYS CFX-Post was used to evaluate and graphically display the results. On the PCs I had Intel i7 and i5 CPUs, on the cluster there were possibility to use 16 CPU of 8 nodes and 32 GB of RAM (2 GB/CPU or 4 GB/node).



8. Results of the model with whole circumference

Selected results got with the model of whole circumference can be seen in the following illustrated by figures.

First, I had a look at the streamlines in the whole computational domain to check the overall characteristics of the flow (see Figure 16). As it can be seen, the streamlines are straight which means that without wrapped wire or other kind of spacers there are not strong inter sub-channel cross flows or other type flow phenomena causing asymmetric flow pattern.

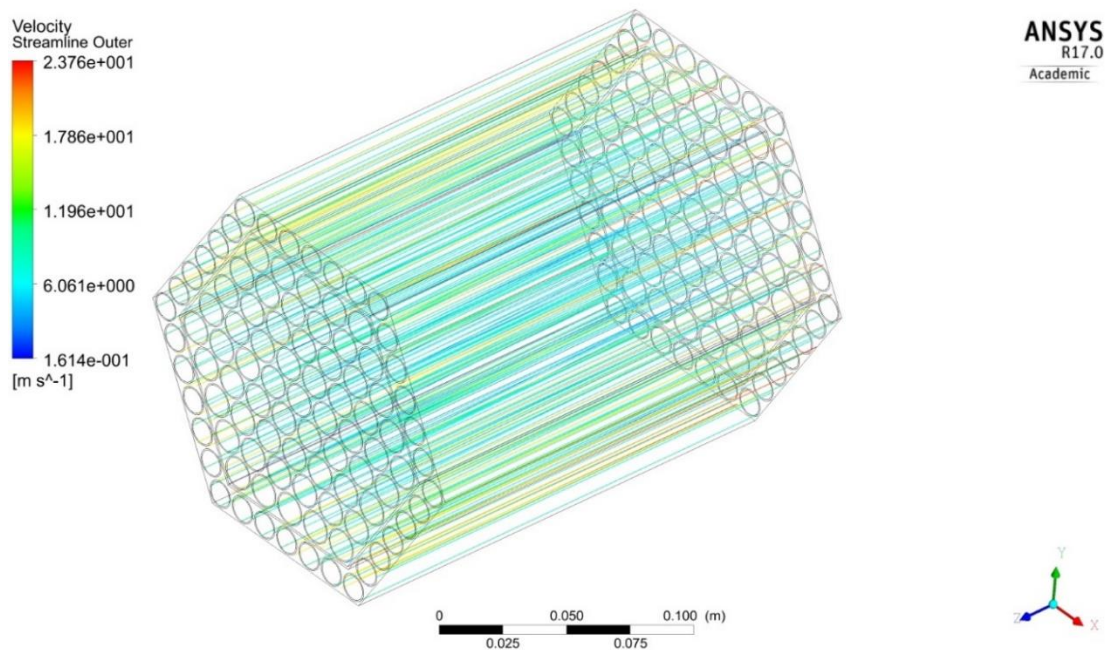


Figure 16: The streamlines in the model with whole circumference

Figure 17 shows the contour plot of mass flow rate at $Z = 0.155$ m height. As it can be seen the mass flow rate in the narrow gaps (between fuel rods or a fuel rod and the internal wall) with decreased cross section is lower, than in the sub-channels with increased cross section. It is very simple to understand: the smaller the cross-section the higher the hydraulic resistance it causes.



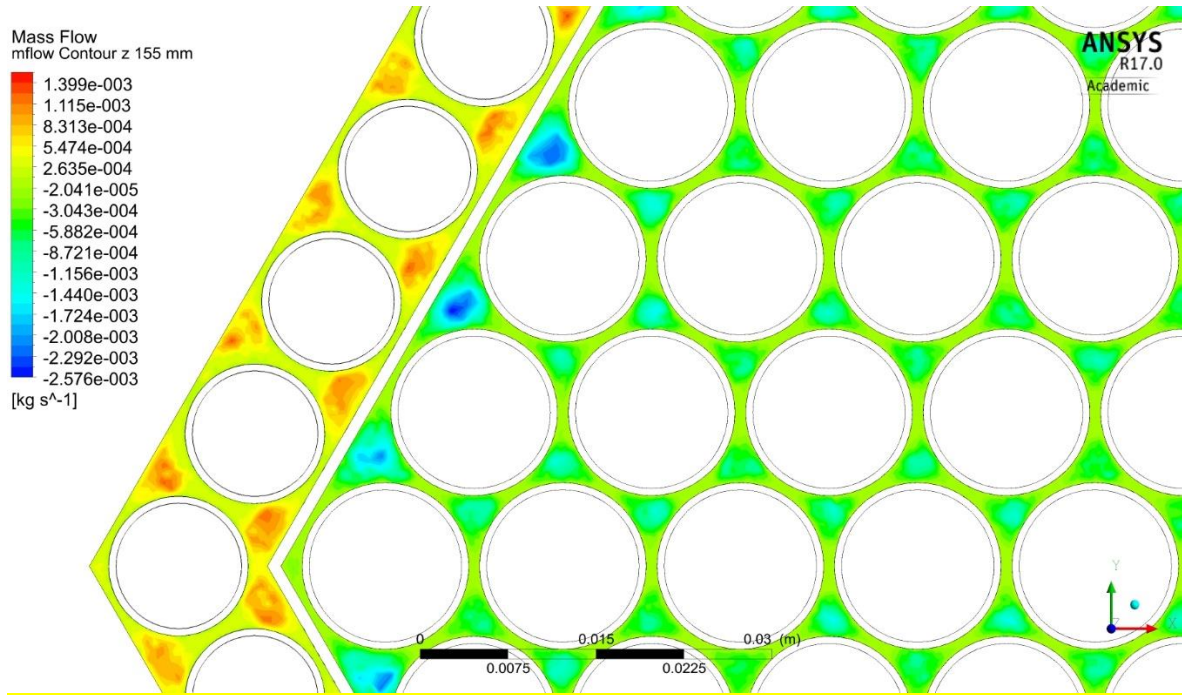


Figure 17: The mass flow rate in a detailed view at 0.155 m axial position

The lower value of mass flow rate causes higher bulk fluid and wall temperatures in the gaps (see Figure 18).

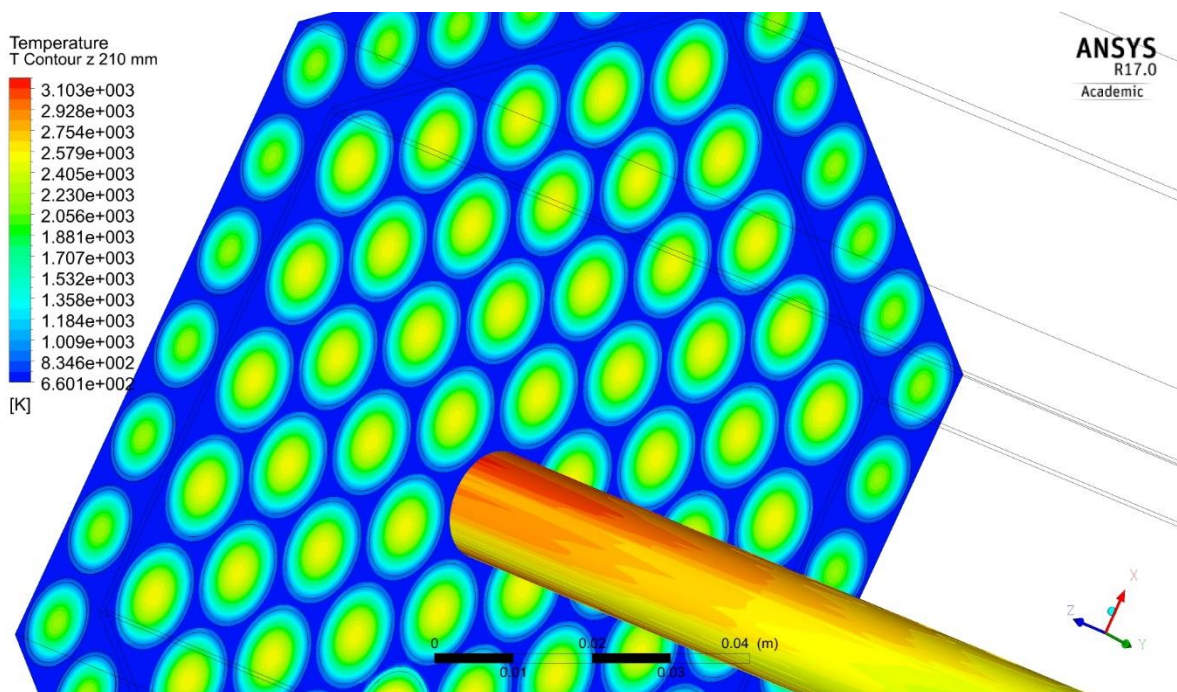


Figure 18: The contour plots of the bulk fluid temperature and the wall temperature on an inner rod

About the wall temperature on the outer surface of the claddings can be stated, that the hottest parts can be found in the upper region of the model (see Figure 18). These hottest parts



occur where the flow is slower (in the gaps between fuel rods and between fuel rod and the internal wall).

The pressure drop in the inner SCW domain was 3400 Pa while it was 11,700 Pa in the outer SCW domain. The difference between the pressure drops of the two fluid domains comes from the difference of the areas and shapes of the two cross sections. The cross section of the outer SCW domain is smaller and tighter compared to the inner SCW domain.

Beyond the results presented above I have check many other aspects and I can point out that the result coincides with my previous expectations and my physical knowledge.

Due to I did not find any asymmetric flow pattern in the model with whole perimeter, I decided to modify my CFD model. In the next step, I have developed a new model with decreased size in the circumference (one-twelfth instead of whole perimeter), but increased extent in the axial direction (full heated length (4.2 m) instead of 0.21 m).



9. Results of the model with one-twelfth circumference

Below, I present the results of the one-twelfth model calculations through some characteristic features represented by figures.

The velocity field has a local maximum in the middle of the sub-channels, as expected (see Figure 19). Where the hydraulic resistance is bigger, the fluid slows down and heat transfer is worse, mainly in gaps and near to the surface of claddings.

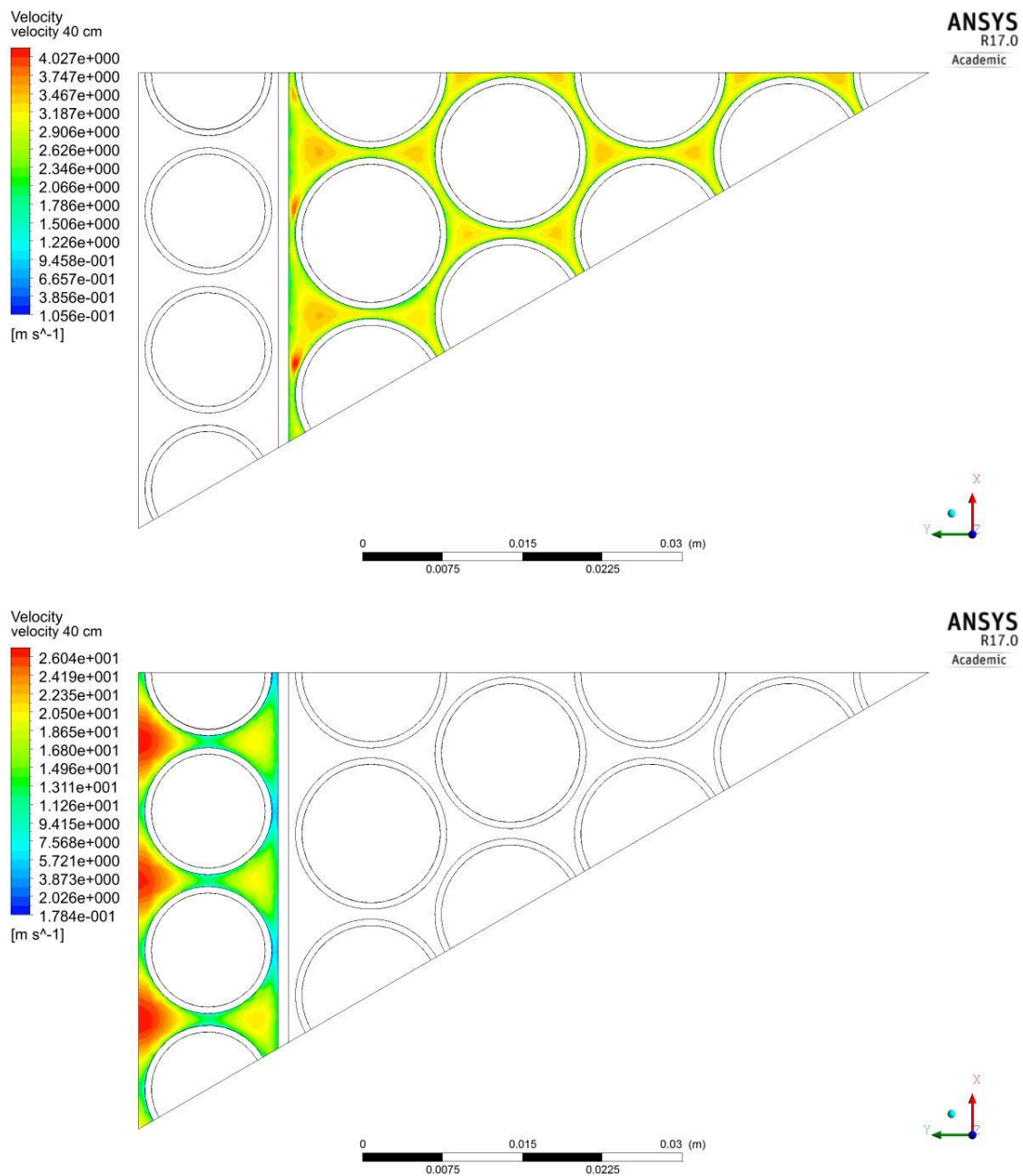


Figure 19: The contour plot of the velocities in the inner (upper) and outer (lower) region at 40 cm axial height



Figure 20 shows the contour plot of the temperature field in all modelled domains (solids and fluids all together). The melting point of the fuel is around 3200-3300°C, which is very close to the maximum temperature of the fuel shown (~2800°C) in Figure 20. It means that a little transient in the normal operation of the reactor or a blockage of a sub-channel by an alien or corrosion product body could lead the melting of the fuel. So, the current design of the fuel assembly has to be modified. This modification can be geometry change (e.g. decrease in the heated length), or redesign of the flow path, or change in the enrichment in the fuel, or change the overall power of the reactor.

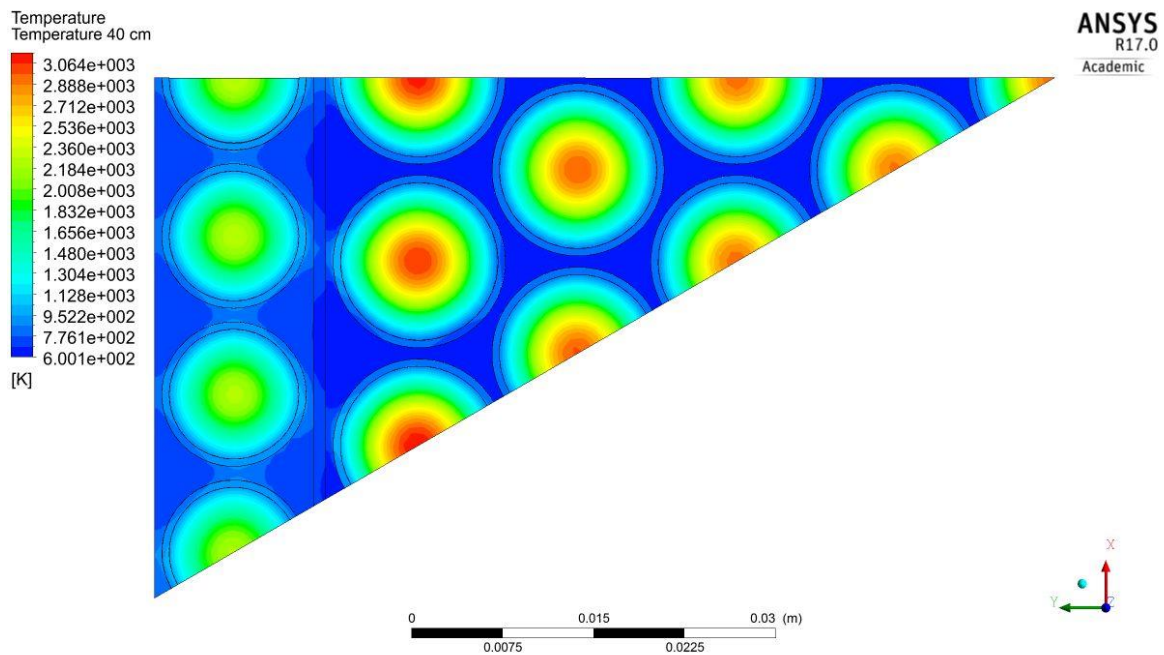


Figure 20: The contour plot of the temperature at 40 cm axial height

Mass flow rate is shown in Figure 21. The negative values are the flows upwards and positive values are the flows downstream. In both fluid domains, these values have a maximum in the middle of the sub-channels, where hydraulic resistance is lower. They have some local maximums in smaller sub-channels and a local minimum in the narrow gaps just like in case of the model with the whole circumference.



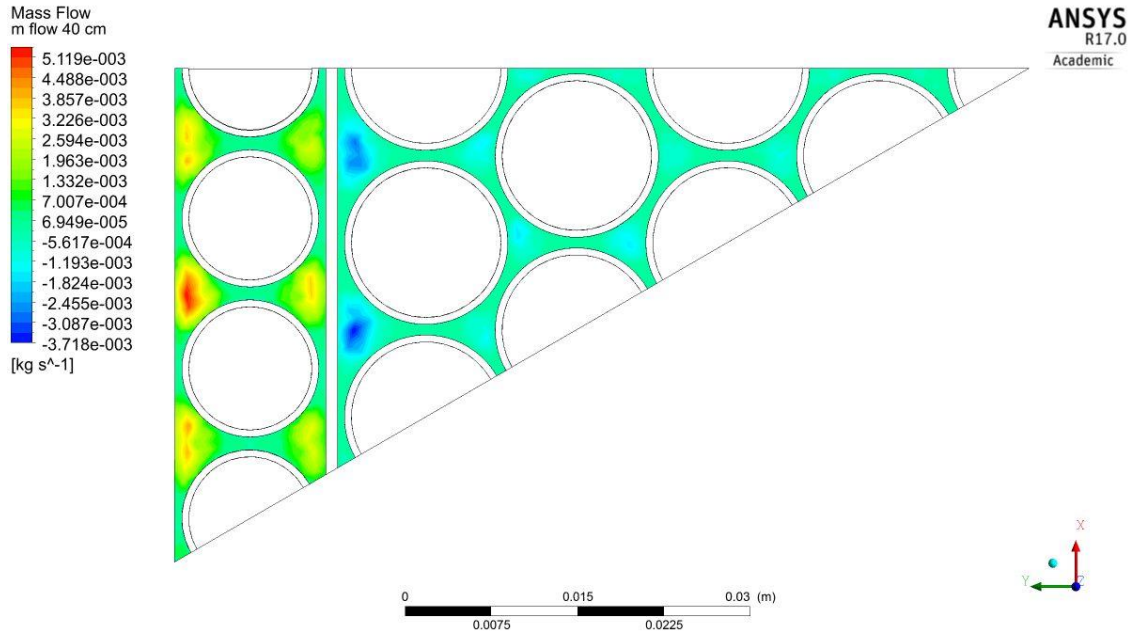


Figure 21: The contour plot of the mass flow rate at 40 cm axial height

Density of water is shown in Figure 22, where we can see the expected pattern. Density has lower values in the narrow gaps where mass flow rate has a minimum and has higher values in the middle of sub-channels due to their lower hydraulic resistance compared to the gaps.

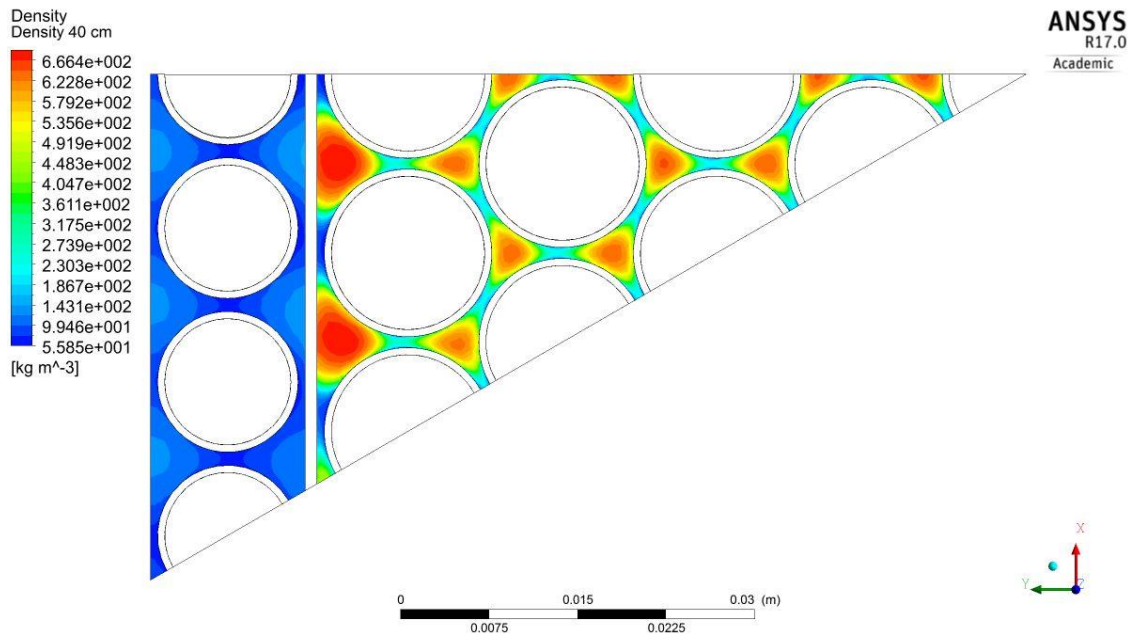


Figure 22: The contour plot of the density of SCW at 40 cm axial height



10. Summary

Thermal hydraulic simulations were carried out to investigate the feasibility of the fuel assembly design of the thorium-SCWR theoretical generation IV reactor concept [18]. This presented work has been performed as the half part of a team work aiming to investigate the feasibility of the concept by a coupled neutronics – 3D CFD code system. I have performed the 3D CFD calculations assisted by the CFD code ANSYS CFX 17.0 version.

I have developed two different CFD models. The computational domain of the first model consists of 21 cm of the heated length and contains the whole circumference of the fuel assembly. The results (e.g. the streamlines) of this model showed that without any spacer device the flow pattern is symmetric, so there was no objection to develop further this model. The second model covered the full length (4.2 m) of the heated part of the fuel assembly, but it modelled only the one-twelfth of the circumference.

One of the main results was that we achieved the connection of the CFX and MCNP codes manually. These modern computer tools allowed us to carry out a precise, fast and reliable analysis of a complex and difficult problem in nuclear engineering. This work is a coordinated application of the advanced tools of computing.

The exchange of calculation results between the CFD analysis and the neutronic calculations was fruitful. The evaluation of heat source density distribution along the heated length showed that this concept in this way is not viable due to the distribution is very strongly bottom peaked. This resulted in a significantly decreased level of heating power in the upper two-third of the heated length.

The second problem which was identified by only the CFD analysis is the very high fuel central temperature ($\sim 2800^\circ\text{C}$). It is close to the melting temperature ($3200\text{-}3300^\circ\text{C}$) of the fuel material. It means that a little transient in the normal operation of the reactor or a blockage of a sub-channel by an alien or corrosion product body could lead the melting of the fuel. Based on this finding, the current design of the fuel assembly has to be modified.

Our first ideas to make this concept feasible: axial profiling the nuclear fuel or shorten the active height of the core. We will move forward and make suggestions how to modify this construction to make this a viable concept.



Bibliography

- [1] https://www.gen-4.org/gif/jcms/c_42151/supercritical-water-cooled-reactor-scwr | Access date: 17. October 2016.
- [2] http://serc.carleton.edu/research_education/equilibria/phaserule.html | Access date: 17. October 2016.
- [3] A.R. Imre, U. K. Deiters, T. Kraska, I. Tiselj, *The pseudocritical regions for supercritical water, Nuclear Engineering and Design* 252 (2012) 179– 183
- [4] Jackson, J. D., *Requirements for similarity in the case of heat transfer to fluids at pressures above the critical value and an approach to the correlation of experimental data. In: Proceedings of 10th UK National Heat Transfer Conference, 10–11 September 2007, Edinburgh, UK*
- [5] S.B. Pope, *Turbulent Flows, Cambridge University Press, 2000.*
- [6] Carmen Isabella Krau, Dietmar Kuhn, Thomas Schulenberg, *Heat Transfer Phenomena of Supercritical Fluids, IYNC 2008, Interlaken, Switzerland, 20 - 26 September 2008, Paper No. 352*
- [7] <http://www.ge.com/in/thermal-power/steam-turbine-manufacturers> | Access date: 17. October 2016.
- [8] Tibor, Reiss (2011), *Coupled Neutronics – Thermal hydraulics Analysis of SCWRs*, Ph.D. thesis
- [9] Sigfred Peterson, R. E. Adams, D.A. Douglas, Jr., *Properties of thorium, its alloys, and its compounds, Oak Ridge National Laboratory, For presentation at the IAEA Panel on "Utilization of Thorium in Power Reactors," Vienna, Austria, June 14-18, 1965.*
- [10] Andrew C. Victor, Thomas B. Douglas, *Thermodynamic Properties of Thorium Dioxide From 298 to 1,200 °K, JOURNAL OF RESEARCH of the National Bureau of Standards-A. Physics and Chemistry, Vol. 65, No.2, March- April 1961*
- [11] Toshiyuki Yamashita, Noriko Nitani, Toshihide Tsuji, Hiromitsu Inagaki, *Thermal expansions of NpO₂ and some other actinide dioxides, Journal of Nuclear Materials* 245 (1997) 72-78.
- [12] R. F. Redmond, J. Lones, *Enthalpies and heat capacities of stainless steel (316), zirconium and lithium at elevated temperatures, Oak Ridge National Laboratory (December 1952)*
- [13] A. Kiss, A. Aszódi, *Summary for Three Different Validation Cases of Coolant Flow in Supercritical Water Test Sections with the CFD Code ANSYS CFX 11.0, Nuclear Technology, Vol. 170/ 1, p. 40-53. (2010)*
- [14] A. Kiss, E. Laurien, A. Aszódi, Y. Zhu, *Numerical simulation on a HPLWR fuel assembly flow with one revolution of wrapped wire spacers, Kerntechnik, 2010/04, Page 148-157.*
- [15] ANSYS Help Viewer, *Version: 17.0.0*
- [16] Tamás, Lajos (2004), *Az áramlástan alapjai, 2008, Page 427.*
- [17] Ványi András Szabolcs (BME TTK III. évf.): „Tórium-urán üzemanyagciklusú SCWR teljesítmény-eloszlásának vizsgálata Monte Carlo módszerrel”, a 2016. évi BME TTK TDK konferenciára benyújtott dolgozat (2016)
- [18] Gy. Csom, T. Reiss, S. Fehér, Sz. Czifrus, *Thorium as an alternative fuel for SCWRs, Annals of Nuclear Energy, Vol. 41, p. 67-78. (March 2012)*

